*Manuscript

Click here to view linked References

A tagged parathyroid hormone derivative as a carrier of antibody cargoes transported by the G protein coupled PTH_1 receptor

Xavier Charest-Morin[a], Jean-Philippe Fortin[b], Robert Lodge[c], Isabelle Allaeys[a], Patrice E. Poubelle[a], François Marceau[a,*]

[a] Centre de recherche en Rhumatologie et Immunologie, CHU de Québec, Québec QC, Canada G1V 4G2

[b] Pfizer's Cardiovascular and Metabolic Diseases Research Unit, Cambridge, MA, USA 02139

[c] Laboratory of Human Retrovirology, Institut de recherches cliniques de Montréal, Montreal, QC, Canada, H2W 1R7

Footnotes:

*Correspondence: Dr F Marceau, CHU de Québec, Centre de Recherche en Rhumatologie et Immunologie, Pavillon CHUL, T1-49, 2705 Laurier Blvd., Québec (Québec), Canada G1V 4G2.

E-mail: francois.marceau@crchul.ulaval.ca

Abstract

Based on the known fact that the parathyroid hormone (PTH) might be extended at its C-terminus with biotechnological protein cargoes, a vector directing the secretion of PTH_{1-84} C-terminally fused with the antigenic epitope myc (PTH-myc) was exploited. The functional properties and potential of this analog for imaging PTH_1R-expressing cells were examined. The PTH-myc construct was recombinantly produced as a conditioned medium (CM) of transfected HEK 293a cells (typical concentrations of 187 nM estimated with ELISAs for PTH). PTH-myc CM induced cyclic AMP formation (10 min), with a minor loss of potency relative to authentic PTH_{1-84}, and c-Fos expression (1-3 h). Treatment of recipient HEK 293a cells transiently expressing PTH_1R with PTH-myc CM (supplemented with a fluorescent monoclonal anti-myc tag antibody, either 4A6 or 9E10) allowed the labeling of endosomal structures positive for Rab5 and/or for β-arrestin$_1$ (microscopy, cytofluorometry). Authentic PTH was inactive in this respect, ruling out a non-specific form of endocytosis like pinocytosis. Using a horseradish peroxidase-conjugated secondary antibody, the endocytosis of the PTH-myc-based antibody complex by endogenous PTH_1R was evidenced in MG-63 osteoblastoid cells. The secreted construct PTH-myc represent a bona fide agonist that support the feasibility of transporting cargoes of considerable molecular weight inside cells using arrestin and Rab5-mediated PTH_1R endocytosis. PTH-myc is also transported into cells that express PTH_1R at a physiological level. Such tagged peptide hormones may be part of a cancer chemotherapy scheme exploiting a modular cytotoxic secondary antibody and the receptor repertoire expressed in a given tumor.

Keywords: parathyroid hormone, PTH_1 receptor, osteoblast, receptor-mediated transport.

List of abbreviations

CM, conditioned medium; mCherry, mCherry fluorescent protein; EGFP: enhanced green fluorescent protein; GPCR, G protein coupled receptor; HRP, horseradish peroxidase; PTH, parathormone; PTH_1R, parathormone receptor 1; TSA: Tyramide Signal Amplification.

Introduction

The parathyroid hormone (PTH) is an 84 aminoacid peptide that is a major regulator of bone metabolism and calcium ion handling by tissues via its "class B," G protein coupled PTH_1 receptor (PTH_1R) expressed in kidneys and the skeleton [14]. Synthetic PTH and its PTH_{1-34} fragment (teriparatide) are currently therapeutically used for an anti-osteoporosis effect [21] and the osteoblast is believed to be their site of action. Furthermore, in a recently reported preclinical model of joint trauma relevant for the physiopathology of osteoarthritis, systemically administered PTH_{1-34} was further proposed to be chondroprotective and chondroregenerative via PTH_1Rs upregulated in chondrocytes [18]. Indeed, PTH is anabolic for cartilage and the serum concentration of the hormone is correlated to cartilage metabolic activity (leucine and sulfate incorporation) in juvenile mice [24]. Further, PTH_1R is expressed in various tumor cells [13,17]. PTH_1R is subjected to agonist-induced, β-arrestin-dependent internalization [9].

Recent crystal structures of agonist-bound PTH_1R extracellular domain revealed that the C-terminal hormone residue does not form direct contacts with the receptor [16]. This made possible two recent biotechnological forms of PTH_{1-34}-based agonists elongated at their C-terminus, either with a linker and trans-membrane tether in one case [6,7], or in the other, with the green fluorescent protein (GFP), leading to a high molecular weight probe suitable for imaging studies in cells that express recombinant PTH_1R [3] (schematic representation, Fig. 1A, structure (a)). Here, we evaluated a vector that directs the secretion of the full PTH_{1-84} sequence conjugated at its C-terminus with 2 antigenic tags, including the myc epitope (Fig. 1B), as this construction may be the basis of the modular construction of even larger cargoes based on anti-myc antibodies (Fig. 1A(b-c)). These novel agonist constructs were evaluated for their imaging potential in cells expressing recombinant or natural PTH_1Rs. PTH-myc is part of a growing set of myc-tagged agonist peptide hormones that transport antibodies into cells via arrestin-mediated GPCR cycling (bradykinin B_2 receptor [8]; CC-chemokine receptor 7 [4]).

Materials and methods

Cell culture, transfection and analysis

A subclone of HEK 293 cells, called HEK 293a, originally obtained from Sigma-Aldrich was used in most experiments. This cell type was grown in Dulbelcco's modified Eagle's medium supplemented with 10 % FBS, 1 % L-glutamine and 1 % penicillin-streptomycin stock solutions (100 ×). The cells were used as recipients of a vector purchased from OriGene Technologies (Rockville, MD): myc-DDK-tagged pro-PTH, that directs the secretion of the mature human PTH_{1-84} sequence extended at its C-terminus with 2 epitopes in tandem, myc and DDK (catalog number RC519848; translated amino acid sequence in Fig. 1). The latter construction will be conventionally designated as PTH-myc. Seventy % confluent producer cells were transfected with a given vector using the ExGen reagent (Fermentas) used as directed.

Other recipient HEK 293a cells were grown and transiently transfected as described above with a vector coding for PTH_1R (gift from Dr. T. J. Gardella, Massachusetts General Hospital), and were further optionally co-transfected with mCherry fluorescent protein (mCherry), Rab5-mCherry, Rab5-GTP-locked-mCherry, Rab7-mCherry (given by Dr. M. J. Tremblay, Université Laval, Canada), or β−arrestin$_1$-mCherry (kind gift from Dr. J.-M. Beaulieu, Université Laval, Canada). Stimulations for microscopic or cytofluorometric experiments were based on the CM of the PTH-myc construction was supplemented with Alexa-Fluor-488-conjugated monoclonal antibodies (clone 4A6, Millipore, dilution 1:1000 corresponding to a final antibody concentration of approximately 3.3 nM in the culture medium). The alternate anti-myc tag monoclonal antibody 9E10 conjugated with Alexa-Fluor-488 was also used in microscopy (Millipore, dilution 1:1000). Cells were generally treated for 30 min with stimulants (incubation carried out at 37°C in humidified atmosphere containing 5% CO_2), rinsed 3 times with phosphate buffered saline, observed in microscopy for epifluorescence and photographed using an Olympus BX51 microscope coupled to a CoolSnap HQ digital camera (filters for AlexaFluor-488: excitation 460-500 nm, emission 510-560 nm; for mCherry fluorescent protein: excitation 525-555 nm, emission 600-660). The objective lens was generally the 100× oil UPlanApo (Olympus). This system has a thin focal depth in the relatively thick HEK 293a cells, supporting co-localization studies in a satisfactory manner. An alternate stimulant was PTH_{1-84} (Sigma-Aldrich). Other transfected cells were detached using the protease-free Cell Dissociation Buffer (Invitrogen), incubated in D-MEM without serum at 37°C for 30 min under agitation in the presence of a stimulant, rapidly centrifuged (30 sec, 11,000 g) and resuspended in phosphate buffered saline. Then, the fluorescence of the cell suspensions was assessed using the BD SORP LSR II cell analyzer for the uptake of a green fluorophore as a function of stimulation and transgene expression.

Detection of endogenously expressed PTH_1R using the endocytosis of PTH-myc-anti-myc antibody complexes

The antibody cargo system has been adapted to detect PTH_1R-mediated transport in relevant cells and also in HEK 293a expressing recombinant PTH_1R, for comparison. The human osteoblastoid cells MG-63, originally obtained from the ATCC and propagated in α-MEM supplemented with 10% fetal bovine serum, antibiotics and L-glutamine, was also used in some experiments. Cells have been incubated for 30 min (37°C) in the PTH-myc or control CM supplemented with the non-labeled 4A6 monoclonal antibody (Millipore, final concentration ≈ 3.3 nM). Then, cells were fixed, permeabilized and stained with the Tyramide Signal Amplification (TSA) Kit containing horseradish peroxidase (HRP) conjugated goat anti-mouse IgG antibodies and AlexaFluor-488-tyramide as a fluorogenic co-substrate of the reaction (Invitrogen kit T20912 used as directed). The TSA technology applied to immunohistochemistry is reviewed elsewhere [23].

Immunoblots

The agonist action of PTH-related agonists was investigated using the expression of the transcription factor c-Fos, a distal signaling response to the stimulation of various receptor-ligand systems [10]. Total HEK 293a cell extracts were immunoblotted to detect c-Fos expression using the K-25 rabbit polyclonal antibodies (Santa Cruz Biotechnology; dilution 1:100).

ELISA of cyclic AMP and PTH

A commercial cyclic AMP ELISA kit (Cell Biolabs, San Diego, CA) was applied as directed without the optional acylation reaction to quantify the intracellular second messenger of PTH_1R-expressing HEK 293a cells (confluent 35-mm petri dishes) variously stimulated. Another ELISA kit, the Intact Parathyroid Hormone ELISA Kit (GenWay Biotech, San Diego, CA) was used to quantify PTH-myc in CM (dilution 1:10 – 1:200). This assay sequentially exploits antibodies directed to both the N- and C-terminal regions of human $PTH_{1\text{-}84}$ and, therefore, is selective for the whole sequence peptide.

Data analysis

Numerical values are reported as means ± s.e.m. Non-normally distributed groups of values were analyzed using nonparametric analysis of variance (Kruskal-Wallis test) followed by Dunn's multiple comparison test. Normal sets of values were compared using ANOVA followed by Tukey-Kramer multiple comparison test or, for comparison with a common control value, Dunnett’s test (InStat 3.05 computer program, GraphPad Software; San Diego, CA).

Results

Characterization of PTH-myc as carrier of an antibody cargo: visualization tool

The CM of HEK 293a cells transiently transfected with the vector coding for the tagged protein PTH-myc contained the equivalent of 187 ± 15 nM of PTH (ELISA for full sequence PTH, n = 3). The control CM of untransfected cells did not contain measurable immunoreactive PTH (n = 2). In acute tests (10-min stimulation), PTH-myc was about 4-fold less potent than PTH_{1-84} to raise cyclic AMP in HEK 293a cells that expressed recombinant PTH_1R (ELISA determinations, Fig. 2). The c-Fos expression and extensive phosphorylation (detected as an increasing ladder of immunoreactive proteins) induced by PTH-myc CM were much more intense than that produced by 10 nM synthetic PTH_{1-84} (Figure 3), consistent with the higher immunoreactive hormone concentration in the CM. The fact that multiple bands are detected with the anti-cFos antibody may also derive from certain cross-reactivities with the c-Fos homologues Fos B and Fra-2, according to the antibody manufacturer. c-Fos signaling was persistent, as both forms of stimulation had declining but detectable effects after 12 h. In experiments reported in Figures 2 and 3, synthetic PTH_{1-84} was added to the serum-containing culture medium, thus supporting reasonable comparisons with PTH-myc present in the CM.

Experiments were designed to evidence the PTH_1R-mediated cellular uptake of immune complexes formed in the culture medium and composed of PTH-myc bound to a fluorescent anti-myc antibody (microscopy, Figure 4, or cytofluorometry, Figure 5). Controls included cells that did not express PTH_1R, cells stimulated with synthetic PTH_{1-84} (10-100 nM) or with the CM of untransfected HEK 293a cells. A very robust and specific endosomal labeling of recipient cells that expressed the receptor was observed (Figure 4). These observations support that the PTH-myc-4A6 (Fig. 4A) or PTH-myc-9E10 immune complexes (Fig. 4B) formed in the culture medium were recognized by the PTH_1R as agonists and were transported into endosomes. Cytofluorometry confirmed these results (based on the fluorescent 4A6 antibody, Figure 5). Of note, synthetic PTH_{1-84} devoid of the myc epitope was not competent to induce the endocytosis (pinocytosis) of droplets of the culture medium containing the fluorescent antibody (Figures 4 and 5), further supporting the specific molecular interaction of the myc-tagged agonist with the antibody. Receptor-expressing cells co-treated with the PTH-myc-4A6 immune complexes and with synthetic PTH_{1-84} (150 nM or 1.52 μM) evidenced concentration-dependent competition for endocytosis of the fluorescent antibody by an excess of the unlabeled agonist (Fig. 4C).

The PTH-myc/4A6 costimulation scheme supported β-$arrestin_1$ colocalization studies (Figure 6, top). The mCherry-tagged arrestin is homogeneously expressed in the cytosol of recipient cells that co-expressed PTH_1R. Both PTH_{1-84} and the CM of PTH-myc induced the condensation of β-$arrestin_1$-mCherry into endosomal structures, but only the myc-tagged agonist carried with it the fluorescent antibody that was extensively colocalized with condensed β-$arrestin_1$-mCherry (Figure 6). Thus, tetramolecular complexes must be detected at the endosomal level: antibody-agonist-receptor-arrestin, with the first and fourth molecules only being fluorescent. Colocalization of the PTH-myc-fluorescent anti-myc antibody complex was also tested in cells expressing the receptors and one of two Rab5-mCherry constructions: the GTP-locked activated form that causes the formation of giant endosomes [19] or the wild type one (Figure 7): colocalization was extensive in cells treated for 30 min with the CM of PTH-myc. Rab5 is a marker of early endosomes, whereas Rab7 rather labels late endosomes. While the PTH-myc/4A6 did not colocalize with Rab7-mCherry after 30 min of incubation, minor colocalization was observed after 3 or 6 h (Figure 8), indicating a slow progress of the antibody cargo in the endosomal/lysosomal tract.

Application of PTH-myc to imaging of endogenously expressed PTH_1R

In HEK 293a cells that express PTH_1R, but not in control cells, a very bright intracellular signal was detected following endocytosis of the PTH-myc-4A6 antibody complex using the TSA system that enzymatically generates AlexaFluor-488 labeling (Figure 9A). This amplified detection system has been applied to detect the naturally expressed PTH_1R in relevant cells.

The human osteoblastoma MG63 cell line is known to express PTH_1R and to functionally respond in several ways to $PTH_{1\text{-}84}$, $PTH_{1\text{-}34}$ and other ligands [5,11,12,25]. This cell line exhibits a slight but consistent granular uptake of the AlexaFluor-488-conjugated anti-myc antibody if co-treated with PTH-myc CM, but not when exposed to the control CM of HEK 293a cells (microscopy, Figure 9B). The enzymatically amplified TSA detection system, based on a HRP-conjugated secondary antibody, revealed the endocytosis of the 4A6 antibody-PTH-myc complex in a more intense manner with some non-specific nuclear staining (Figure 9B). These experiments establish that the same hierarchy of sensitivities for PTH_1R visualization techniques exists in MG-63 cells as in HEK 293a cells that express recombinant receptors, but lower intensities in the system that expresses low physiological levels of PTH_1R.

Discussion

Because the secretin receptor family is tolerant to variations in the C-terminal structure of peptide ligands [7], we hypothesized that PTH-myc, efficiently secreted and combined in the extracellular milieu with an anti-myc antibody, would support the endocytosis of a very large agonist cargo (in excess of 150 kDa) mediated by recombinant or naturally expressed PTH_1R (Figures 4-10). PTH-myc is a close analog of the full hormone sequence and both increased cellular cyclic AMP (Fig. 2) and exert a prolonged effect on the c-Fos expression assay (Figure 3). The recombinant peptide PTH-myc has been compared to synthetic PTH_{1-84} in the assay of acute cyclic AMP generation (Fig. 3), but not in the slow c-Fos induction assay (Fig. 4), where arbitrary agonist concentrations were used; the former assay evidence only a minor loss of potency in the myc-tagged agonist. Findings suggest that binding of the tagged agonist to the antibody does not impair the recognition of the receptor by PTH_{1-84} and that this design enables protein cargoes even larger than green fluorescent protein [3] to be transported by the activated PTH_1R. The anti-myc 4A6 monoclonal antibody used in the present work has previously been shown to be internalized by the activated bradykinin B_2 receptors, whether the myc epitope was located in the receptor construction or at the N-terminus of a synthetic agonist [2,8], and also by the chemokine receptor CCR7 via a myc-tagged agonist (CCL19-myc) [4]. The alternate 9E10 anti-myc monoclonal antibody was also internalized as a cargo tightly bound to the agonist PTH-myc, despite its more unpredictable behavior *vs.* sequences that flank the myc epitope in protein constructions [1]. We have not exploited the built-in DDK epitope present in the commercial PTH-myc construction (Fig. 1), because a typical commercial anti-DDK tag is both less sensitive and specific than the anti-myc monoclonals in our hands. Importantly, results highlight that detection of the co-endocytosed 4A6 monoclonal antibody using an enzymatically amplified reaction is a powerful visualization aid for the PTH_1R that proved cargo endocytosis by endogenously expressed receptors in the osteoblastoid cells MG-63.

The anti-osteoporosis peptide PTH_{1-34} is inactivated by receptor-expressing cells and has a short duration of action in-vivo; daily administration of this agent leads to a “pulsed” effect on osteoblast that is believed to be obligatory for the desired anabolic effect [22]. The PTH-myc construction is based on the PTH_{1-84} sequence known to undergo massive receptor-mediated endocytosis and that determines slow intracellular cycling relative to the alternate agonist PTH-related peptide (PTHrP) [22]. Further highlighting the complexity of this system, recent evidence supports that non-canonical signaling emerging from endocytosed PTH_1Rs bound to β-arrestins may also impact the relative therapeutic efficacy of these analogs [9,22]. These observations may reflect different cycling and signaling kinetics relative to the parent peptides. Although beyond the scope of the present study (focused on imaging applications), such future analyses will be important to better understand how heavy C-terminal modifications impact the pharmacological properties of emerging class B GPCR agonist therapeutics. For instance, albiglutide is a new anti-diabetic glucagon-like peptide 1 receptor agonist fused to albumin; this fusion protein exhibits considerable alteration of pharmacokinetics relative to the parent peptide [20].

Altering the cargo protein at the C-terminus of the PTH_1R activating sequence could lead to more ambitious applications that are not currently supported by the present study. (1) In relationship to the recently proposed use of a systemically administered PTH_1R agonist in osteoarthritis [18], the present study suggests the possibility to produce alternate high molecular weight agonists adapted to intra-articular injection with decreased systemic diffusion, prolonged signaling and decreased “off target” side effects. (2) Further, a functional cytotoxic protein cargo conjugated to PTH could theoretically be useful to treat malignant chondrosarcomas, where PTH_1R expression is consistently upregulated in a manner correlated with histological grade [17]. PTH_1R is also expressed in an apparently ectopic manner in a number of human carcinomas (e.g., prostate, pancreas) [13]. In such application, a novel generation of anti-myc monoclonal antibodies armed with cytotoxic drugs via acid-labile bonds that are released in endosomes [15] could be targeted to tumor cells that express PTH_1R (as modeled in MG-63 cells). The strategy is modular, being adaptable to other tagged agonists, for instance CCL19-myc, an agonist of CCR7 often expressed in metastatic tumors [4]. The agonist effect of the peptide hormone vector, documented for PTH-myc, would not necessarily be detrimental because the transient stimulation of tumor cell mitosis or metabolism could selectively increase their sensitivity to anti-mitotic drugs conjugated to the secondary antibody.

Possessing an intact N-terminal receptor-binding sequence, the construction PTH-myc is a *bona fide* bifunctional agonist that shows the feasibility of the transport of cargoes of considerable molecular weight by PTH_1R. The sensitive detection of PTH_1R using the tagged agonist, primary anti-tag antibody and secondary HRP-conjugated antibody may rivals the immunohistochemistry based on an anti-PTH_1R monoclonal antibody [13], but is potentially applicable to multiple animal species, because the agonist effect of peptide hormones may cross the species barrier more easily than the reactivity of anti-receptor antibodies. Considering the structural similarities between class B1 GPCR hormones, it may be anticipated that additional peptides belonging to this family will show useful pharmacologic properties when conjugated to antigenic tags for imaging purposes or tissue-specific delivery of biotechnological cargoes.

Acknowledgements

This work was supported by the grant MOP-93773 from the Canadian Institutes of Health Research (CIHR), by Successive Fellowship Awards to J.-P. F. from the CIHR and the Fonds de la Recherche en Santé du Québec. We thank Dr. T. J. Gardella (Massachusetts General Hospital, Boston, USA) for the gift of the PTH_1R expression vector, Drs. Michel J. Tremblay and Martin Beaulieu (Université Laval) for the gift of the mCherry labeled vectors (Rabs and β-arrestin$_1$, respectively), Dr. Dr. Marc Pouliot (CHU de Québec) for facilitating the access to microscopic equipment and Dr. Alexandre Brunet for operating the cytofluorometric equipment.

References

[1] Anonymous, 2006. Epitope tagging generates new products. Gen Engineer Biotechnol News 2006;26:1812-4.

[2] Bawolak MT, Lodge R, Morissette G, Marceau F. Bradykinin B_2 receptor-mediated transport into intact cells: anti-receptor antibody-based cargoes. Eur. J. Pharmacol. 2011;668:107-14.

[3] Charest-Morin X, Fortin JP, Bawolak MT, Lodge R, Marceau F. Green fluorescent protein fused to peptide agonists of two dissimilar G protein-coupled receptors: novel ligands of the bradykinin B_2 (rhodopsin family) receptor and parathyroid hormone PTH_1 (secretin family) receptor. Pharmacol Res Persp 2013;1:e00004.

[4] Charest-Morin X, Pépin R, Gagné-Henley A, Morissette M, Lodge R, Marceau F., C-C chemokine receptor-7 mediated endocytosis of antibody cargoes into intact cells. Front Pharmacol 2013;4,122.

[5] Datsis GA, Berdiaki A, Nikitovic D, Mytilineou M, Katonis P, Karamanos NK, Tzanakakis GN. Parathyroid hormone affects the fibroblast growth factor-proteoglycan signaling axis to regulate osteosarcoma cell migration. FEBS J. 2011;278:3782-92.

[6] Fortin JP, Chinnapen D, Beinborn M, Lencer W, Kopin AS. Discovery of dual-action membrane-anchored modulators of incretin receptors. PLoS ONE 2011;6:e24693.

[7] Fortin JP, Zhu Y, Choi C, Beinborn M, Nitabach MN, Kopin AS. Membrane-tethered ligands are effective probes for exploring class B1 G protein-coupled receptor function. Proc Natl Acad Sci USA 2009;106, 8049-54.

[8] Gera L, Roy C, Marceau F. Bifunctional epitope-agonist ligands of the bradykinin B_2 receptor. Biol. Chem. 2013;394:379-83.

[9] Gesty-Palmer D, Luttrell LM. 'Biasing' the parathyroid hormone receptor: a novel anabolic approach to increasing bone mass? Br J Pharmacol 2011;164:59-67.

[10] Glauser DA, Schlegel W. Sequential actions of ERK1/2 on the AP-1 transcription factor allow temporal integration of metabolic signals in pancreatic β cells. FASEB J 2007;21:3240-9.

[11] Kim BG, Park YJ, Libermann TA, Cho JY. PTH regulates myleoid ELF-1-like factor (MEF)-induced MAB-21-like-1 (MAB21L1) expression through the JNK1 pathway. J Cell Biochem 2011;112:2051-61.

[12] Luo XH, Liao EY, Su X, Wu XP. Parathyroid hormone inhibits the expression of membrane-type matrix metalloproteinase-1 (MT1-MMP) in osteoblast-like MG-63 cells. J Bone Min Metab 2004;22:19-25.

[13] Lupp A, Klenk C, Röcken C, Evert M, Mawrin C, Schulz S. Immunohistochemical identification of the PTHR1 parathyroid hormone receptor in normal and neoplastic human tissues. Eur J Endocrinol 2010;162:979-986.

[14] Mannstadt M, Jüppner H, Gardella TJ, Mannstadt M, Jüppner H, Gardella TJ., 1999. Receptors for PTH and PTHrP: their biological importance and functional properties. Am J Physiol 1999;277:F665-75.

[15] Panowski S, Bhakta S, Raab H, Polakis P, Junutla JR. Site specific antibody drug conjugates for cancer therapy. mAbs 2014;6:34-45.

[16] Pioszak AA, Parker NR, Gardella TJ, Xu HE. Structural basis for parathyroid hormone-related protein binding to the parathyroid hormone receptor and design of conformation-selective peptides. J. Biol. Chem. 2009;284: 28382-91.

[17] Rozeman LB, Hameetman L, Cleton-Jansen AM, Taminiau AH, Hogendoorn PC, Bovée JV. Absence of IHH and retention of PTHrP signalling in enchondromas and central chondrosarcomas. J. Pathol. 2005;205:476-82.

[18] Sampson ER, Hilton MJ, Tian Y, Chen D, Schwarz EM, Mooney RA, Bukata SV, O'Keefe RJ, Awad H, Puzas JE, Rosier RN, Zuscik MJ. Teriparatide as a chondroregenerative therapy for injury-induced osteoarthritis. Sci Transl Med 2011;3:101ra93.

[19] Stenmark H, Parton RG, Steele-Mortimer O, Lütcke A, Gruenberg J, Zerial M. Inhibition of rab5 GTPase activity stimulates membrane fusion in endocytosis. EMBO J 1994;13:1287-96.

[20] Tomkin GH. Albiglutide, an albumin-based fusion of glucagon-like peptide 1 for the potential treament of type 2 diabetes. Curr Opin Mol Ther 2009;11:579-88.

[21] Vescini F, Grimaldi F. PTH 1-84: bone rebuilding as a target for the therapy of severe osteoporosis. Clin Cases Min Bone Metab 2012;9:31-6.

[22] Vilardaga JP, Gardella TJ, Wehbi VL, Feinstein TN. Non-canonical signaling of the PTH receptor. Trends Pharmacol Sci 2012;33:423-31.

[23] von Wasielewski R, Mengel M, Gignac S, Wilkens L, Werner M, Georgii A. Tyramine amplification technique in routine immunohistochemistry. J Histochem Cytochem 1997;45:1455-9.

[24] Weiss A, Linve E, Bernheim J, Silbermann M. Structural and metabolic changes characterizing the aging of various cartilage in mice. Mech Ageing Dev 1986;35:145-60.

[25] Yamamoto T, Kambe F, Cao X, Lu X, Ishiguro N, Seo H. Parathyroid hormone activates phosphoinositide 3-kinase-Akt-Bad cascade in osteoblast-like cells. Bone 2007;40:354-9.

Figure legends

Figure 1. A. Schematic representation of the PTH_1R and its bifunctional agonist ligands that carry cargoes of increasing molecular masses. (a) PTH_{1-34}-EGFP [3]; (b) and (c) PTH_{1-84} tagged with the myc epitope in a C-terminal extension, adapted to transport anti-myc antibody-based cargoes. AF488: AlexaFluor-488 fluorophore; HRP: conjugated horseradish peroxidase. B. Amino acid sequences of successive domains encoded in the PTH-myc vector.

Figure 2. Cyclic AMP production in petri dishes of HEK 293a transiently expressing PTH_1R and acutely (10-min) stimulated as indicated. Results are means of duplicate determinations in a representative experiment out of a set of two.

Figure 3. Induction of c-Fos in HEK 293a cells expressing or not PTH_1R in response to treatments with conditioned media relevant for PTH-myc or PTH_{1-84}. Results representative of 2 experiments.

Figure 4. Endocytosis of anti-myc monoclonal antibodies as determined by co-treatment with the PTH-myc construction in HEK 293a cells that optionally and transiently expressed PTH_1R. The undiluted conditioned media supplemented with antibodies were transferred for a 30-min incubation period at 37°C before rinsing and observation. A. Anti-myc clone 4A6, conjugated to AlexaFluor-488, final concentration in the culture medium 3.3 nM. B. Alternate anti-myc 9E10 clone similarly conjugated. In A and B, control conditioned medium or PTH_{1-84} were used as control stimuli. C. Competition of the endocytosis of the PTH-myc-4A6 immune complexes by co-treatment with unlabeled PTH_{1-84}. Original magnification 1000 ×.

Figure 5. Cytofluorometry of HEK 293a cells that optionally expressed PTH_1R stained with the AlexaFluor-488-conjugated anti-myc monoclonal antibody 4A6. The antibody was added to the culture medium of intact cells along with the indicated co-treatment, undiluted conditioned medium of other cells, some producing PTH-myc, or $PTH_{1\text{-}84}$. Left: distributions based on the counting of 10000 cells. A threshold of autofluorescence was defined using cells treated with the control conditioned medium. It was surpassed only under one set of experimental conditions (arrow). Right: proportion of cells above the threshold under each experimental condition in 3 separate experiments (means ± s.e.m.). ANOVA indicated that the values were heterogeneous ($P<0.01$). * $P<0.01$ vs. controls with or without receptors (Tukey-Kramer multiple comparison test).

Figure 6. Colocalization studies in HEK 293a cells expressing PTH_1R and mCherry-conjugated β-$arrestin_1$. The green signal derives from the endocytosis of the AlexaFluor-488-conjugated anti-myc monoclonal antibody 4A6. Cells were stimulated as indicated for 30 min. Epifluorescence, original magnification: 1000 ×.

Figure 7. Colocalization studies in HEK 293a cells expressing PTH_1R and mCherry-conjugated Rab5 or the GTP-locked variant of the latter. Presentation as in Figure 6.

Figure 8. Colocalization studies in HEK 293a cells expressing PTH_1R and mCherry-conjugated Rab7. Cells were stimulated for variable durations with the conditioned medium of other cells producing PTH-myc. Presentation as in Figure 6.

Figure 9. Detection of recombinant or endogenous PTH_1R using detection of the endocytosed PTH-myc-4A6 antibody complex using the Tyramide Signal Amplification (TSA) system that enzymatically generates AlexaFluor-488 labeling. A. Verification with HEK 293a cells that optionally express the recombinant receptor and were treated with the PTH-myc CM along with the non-fluorescent 4A6 antibody (~3.3 nM). B. Application to MG-63 osteoblastoid cells and comparison of the TSA detection with the cell green autofluoresence and to the fluorescence associated with endocytosed AlexaFluor-488-conjugated anti-myc antibodies. Epifluorescence and transmission, original magnification: 1000 ×.

Figure 1

Fig. 1

A.

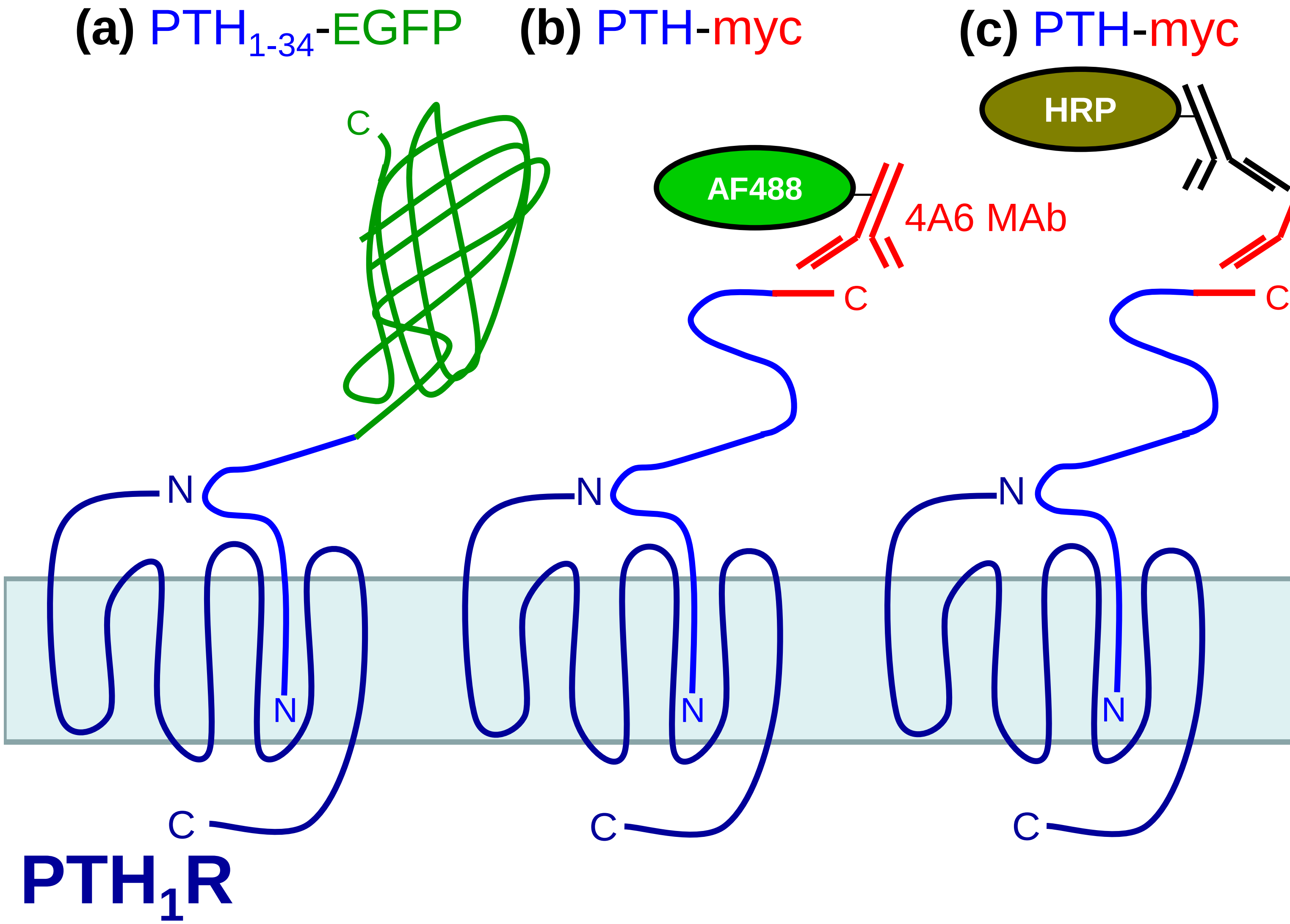

B. **PTH-myc =**

prepro-PTH$_{1\text{-}84}$, human, tagged (OriGene)

MIPAKDMAKVMIVMLAICFLTKSDGKSVKKR
SVSEIQLMHNLGKHLNSMERVEWLRKKLQDVHNFVALGAPLAP
RDAGSQRPRKKEDNVLVESHEKSLGEADKADVNVLTKAKSQ
TRTRPL<u>**EQKLISEEDL**</u>*AANDIL***DYKDDDDKV***stop*

31 first residues = signal peptide
84 next residues = mature PTH
cloning sites + joining peptides
<u>**myc tag**</u>
DDK tag
mature protein 13.0 kDa

Figure 2

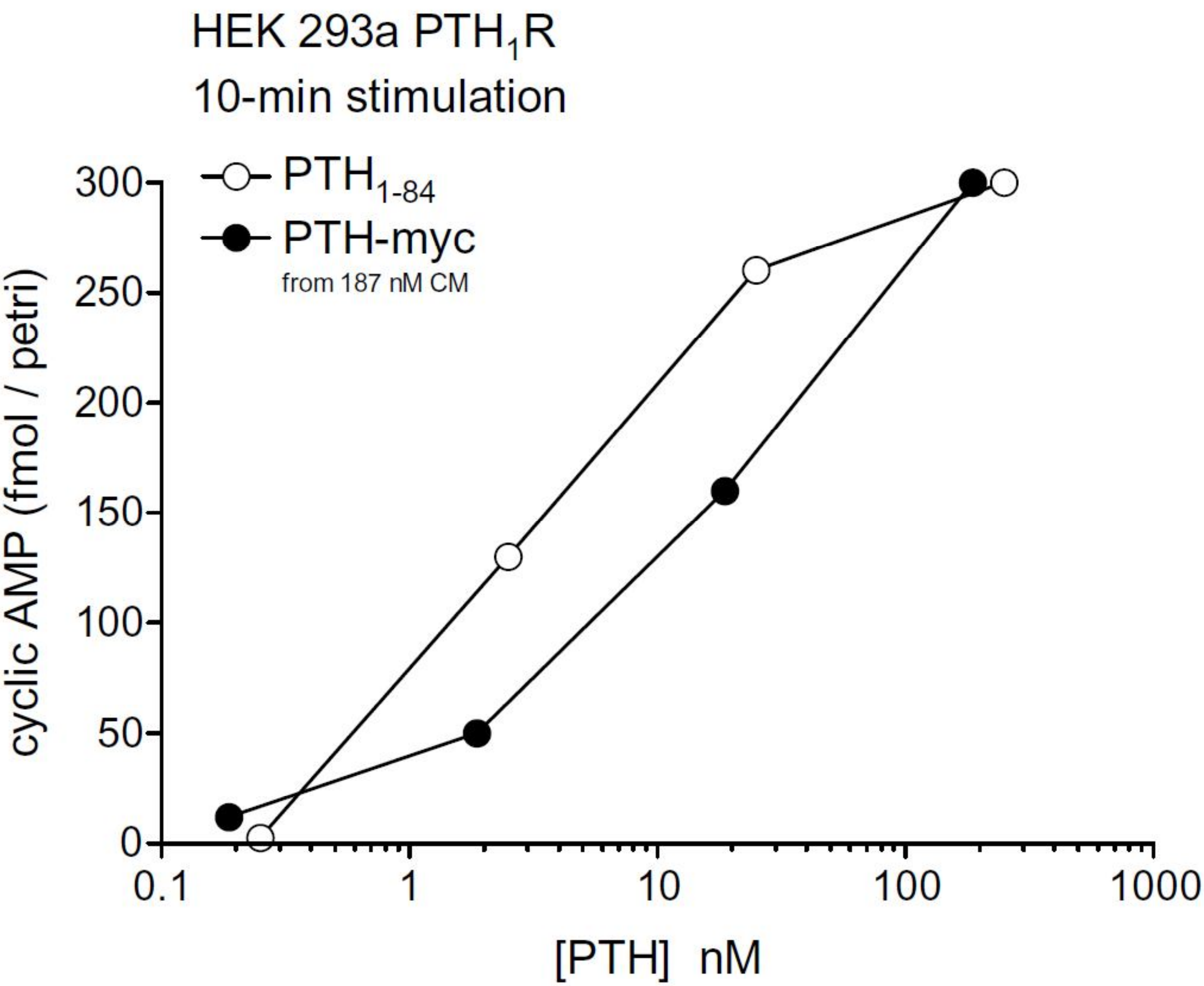
HEK 293a PTH1R
10-min stimulation
PTH1-84
PTH-myc
from 187 nM CM
cyclic AMP (fmol / petri)
300
250
200
150
100
50
0
0.1
1
10
100
1000
[PTH] nM

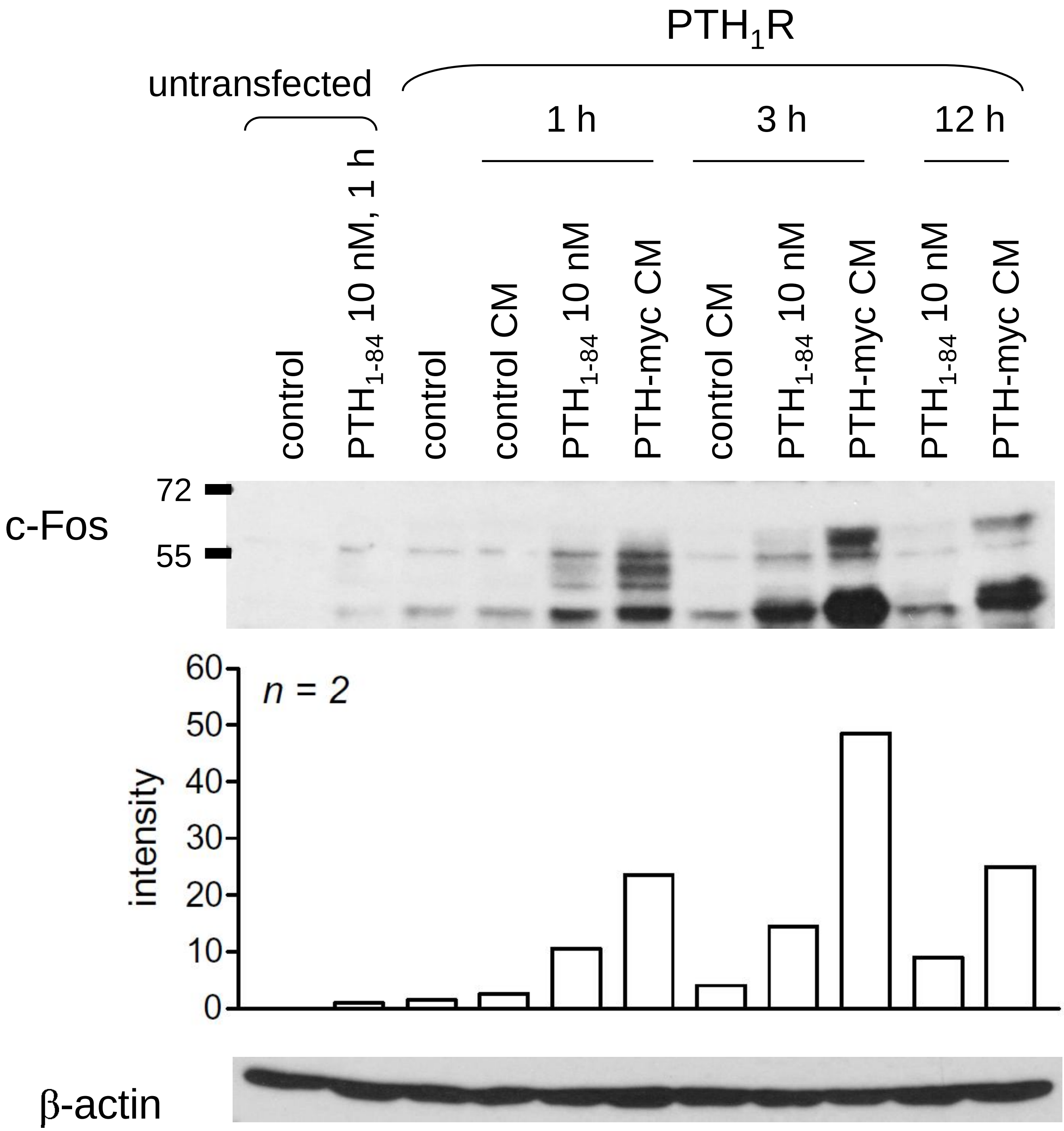

PTH1R
untransfected
1 h
3 h
12 h
control
PTH1-84 10 nM, 1 h
control
control CM
PTH1-84 10 nM
PTH-myc CM
control CM
PTH1-84 10 nM
PTH-myc CM
PTH1-84 10 nM
PTH-myc CM
c-Fos
72
55
60
50
40
30
20
10
0
intensity
n = 2
β-actin

Figure 4

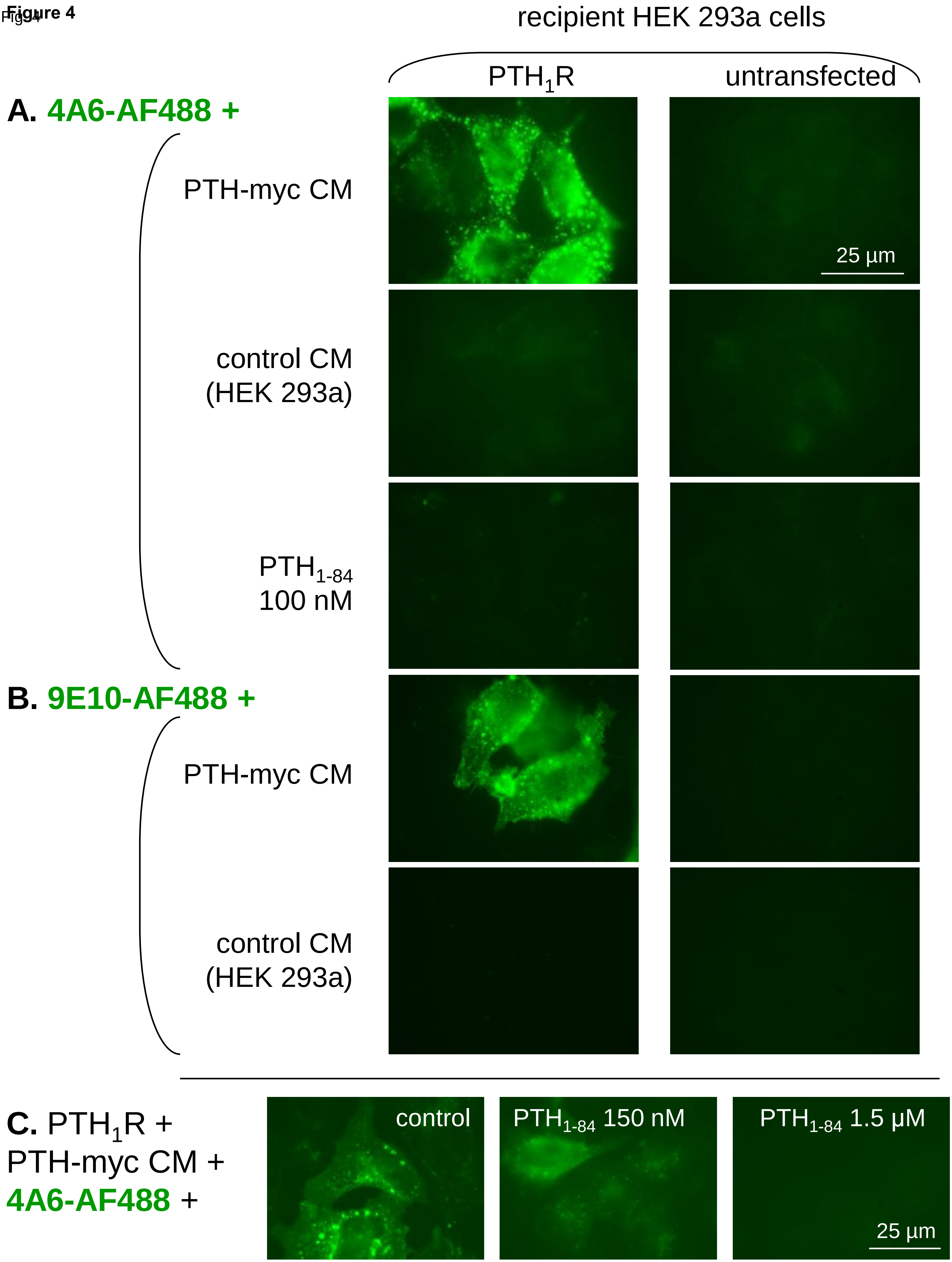

recipient HEK 293a cells
PTH$_1$R
untransfected
A. 4A6-AF488 +
PTH-myc CM
25 µm
control CM (HEK 293a)
PTH$_{1-84}$ 100 nM
B. 9E10-AF488 +
PTH-myc CM
control CM (HEK 293a)
C. PTH$_1$R + PTH-myc CM + 4A6-AF488 +
control
PTH$_{1-84}$ 150 nM
PTH$_{1-84}$ 1.5 µM
25 µm

Figure 5

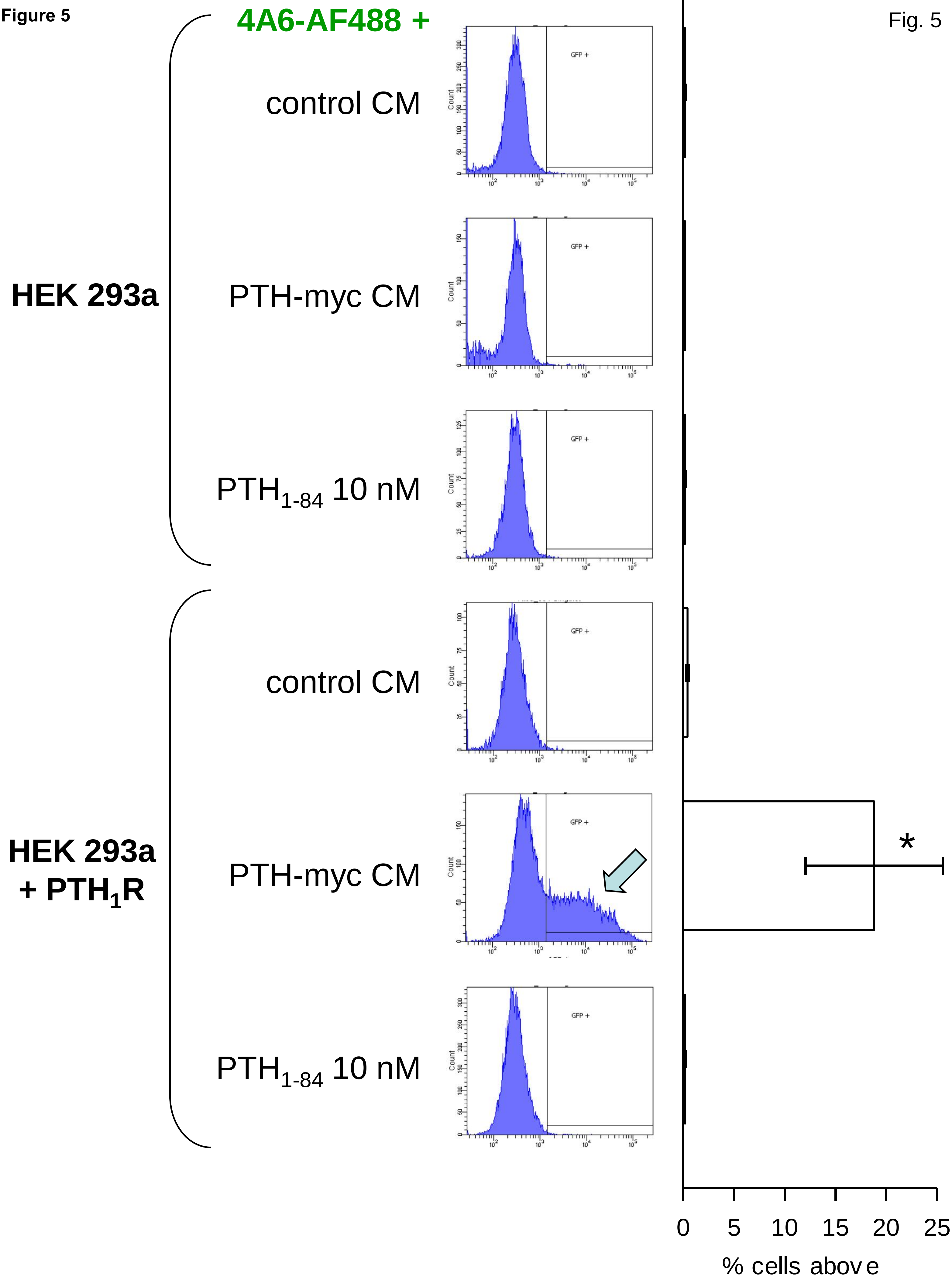
Fig. 5
4A6-AF488 +
HEK 293a
control CM
PTH-myc CM
PTH1-84 10 nM
HEK 293a + PTH1R
control CM
PTH-myc CM
PTH1-84 10 nM
GFP +
Count
*
0
5
10
15
20
25
% cells above

Figure 6
Fig. 6

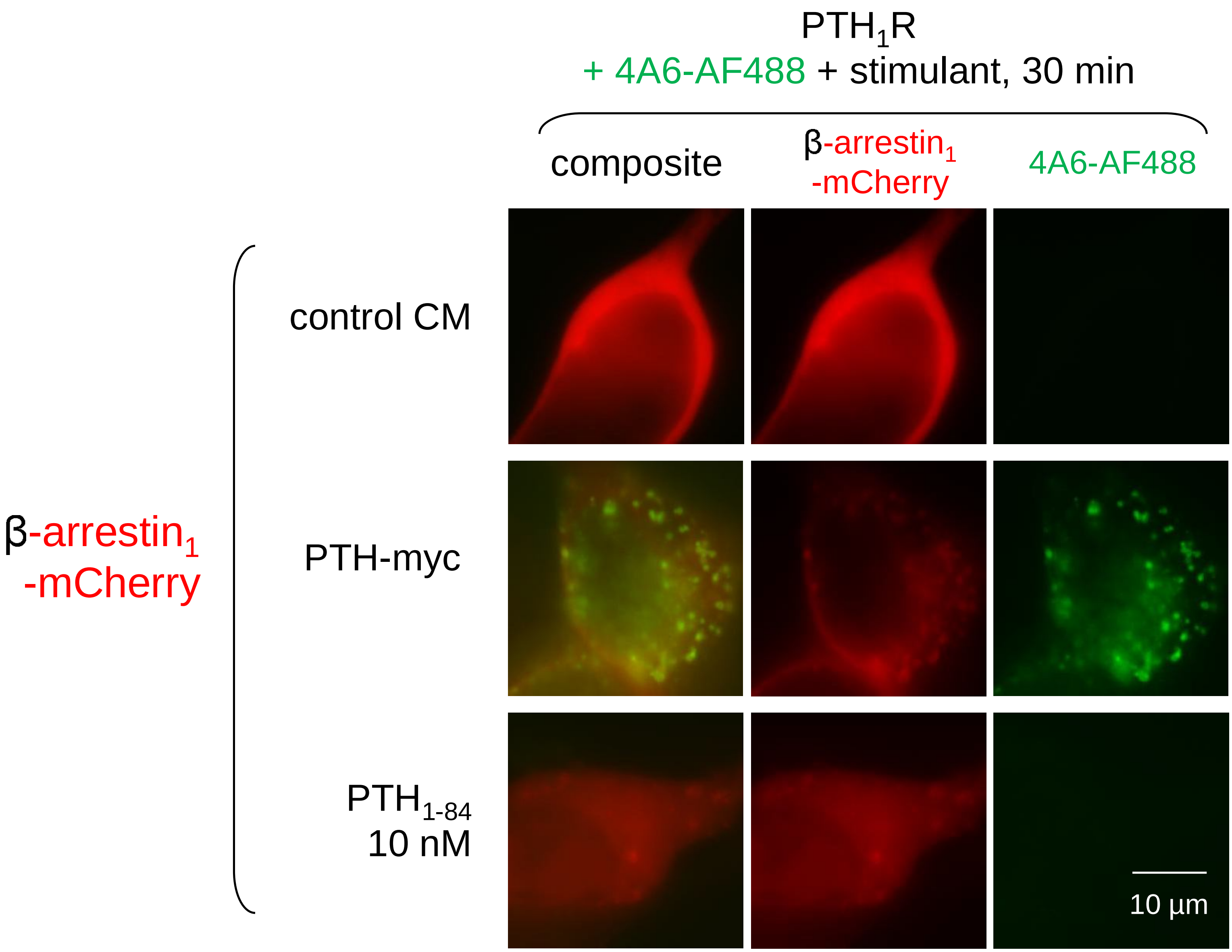

Figure 7

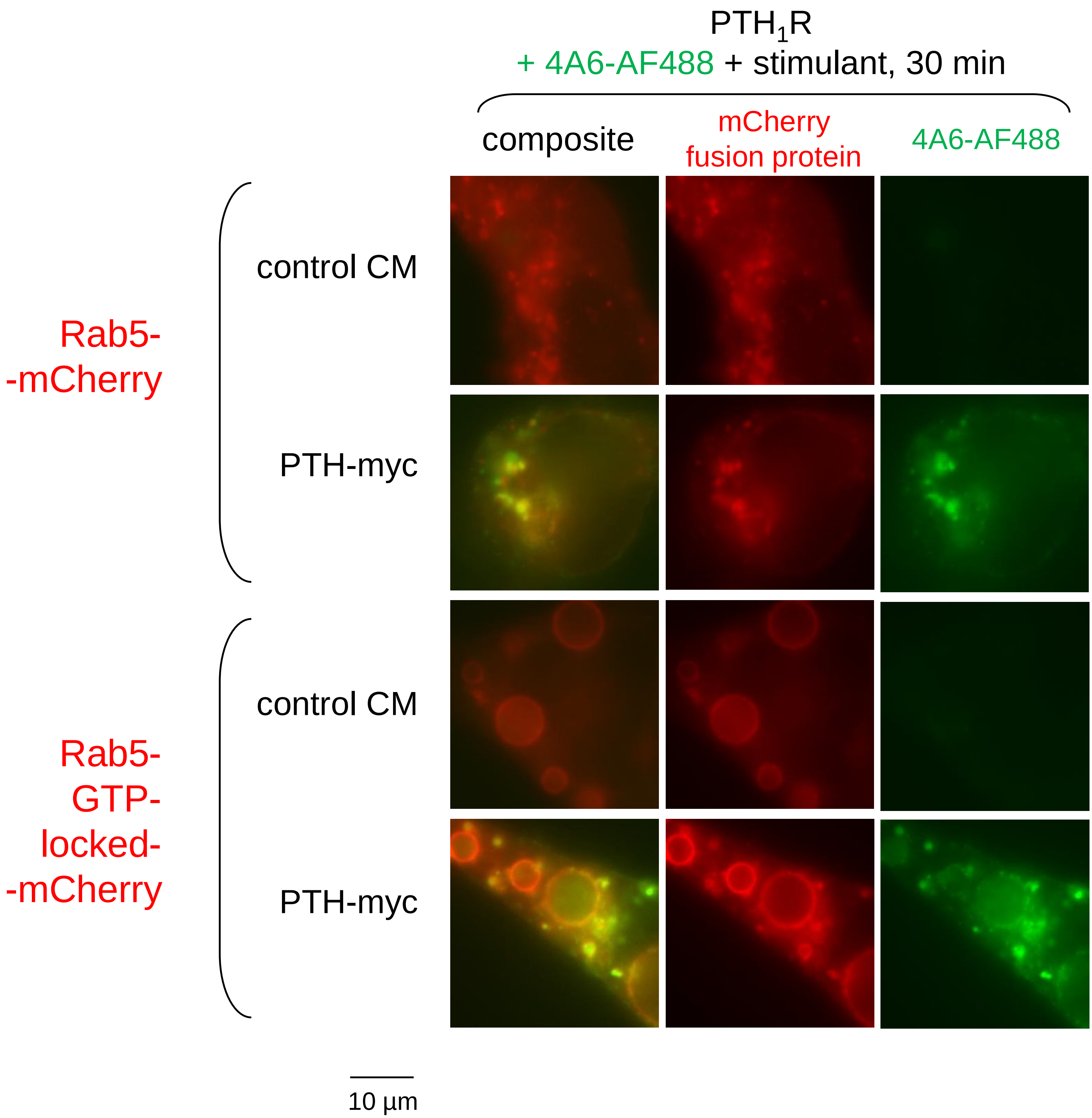

PTH$_1$R
+ 4A6-AF488 + stimulant, 30 min
composite
mCherry fusion protein
4A6-AF488
Rab5-
-mCherry
control CM
PTH-myc
Rab5-
GTP-
locked-
-mCherry
control CM
PTH-myc
10 µm

Figure 8

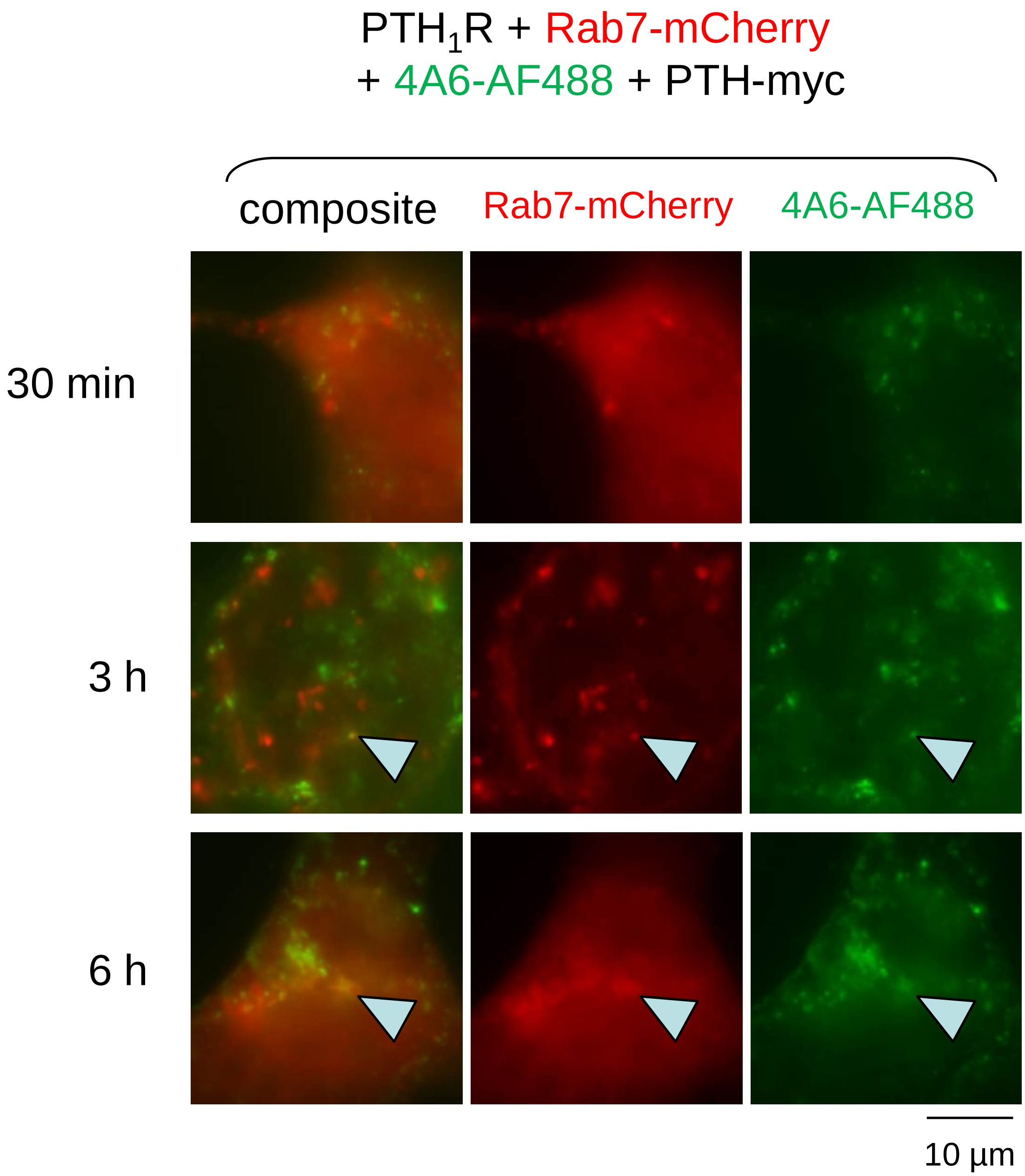

PTH1R + Rab7-mCherry
+ 4A6-AF488 + PTH-myc
composite
Rab7-mCherry
4A6-AF488
30 min
3 h
6 h
10 µm

Figure 9

Fig. 9